TWENTY FIRST EUROPEAN ROTORCRAFT FORUM

Paper No II. 7

A HYBRID NUMERICAL OPTIMIZATION TECHNIQUE BASED ON GENETIC AND FEASIBLE DIRECTION ALGORITHMS FOR MULTIPOINT HELICOPTER ROTOR BLADE DESIGN

A. Rocchetto
Aerodynamic and Flight Mechanic Department
Agusta
Cascina Costa di Samarate (Va), Italy

C. Poloni
Energetic Department
Università degli Studi di Trieste
Trieste, Italy

August 30 - September 1, 1995
SAINT - PETERSBURG, RUSSIA

Paper nr.: II.7

A Hybrid Numerical Optimization Technique Based on Genetic and Feasible Direction Algorithms for Multipoint Helicopter Rotor Blade Design.

A. Rocchetto; C. Poloni

TWENTY FIRST EUROPEAN ROTORCRAFT FORUM
August 30 - September 1, 1995 Saint-Petersburg, Russia

A HYBRID NUMERICAL OPTIMIZATION TECHNIQUE BASED ON GENETIC AND FEASIBLE DIRECTION ALGORITHMS FOR MULTIPOINT HELICOPTER ROTOR BLADE DESIGN

A. Rocchetto
Aerodynamic and Flight Mechanic Department
Agusta
Cascina Costa di Samarate (Va), Italy

C. Poloni
Energetic Department
Università degli Studi di Trieste
Trieste, Italy

Abstract

A tool for helicopter rotor blade design to improve performance and reduce rotor dynamic loads as well as aeroacoustic noise is presented. The optimization procedure is based on a genetic algorithm and a feasible direction technique. The former is used as a global optimizer, whereas the latter is used to refine the solution. The comprehensive analysis codes used to compute rotor performance, noise and loads are an Agusta proprietary code and CAMRAD/JA. Applications of this methodology to a twin engine light helicopter in different operative conditions are illustrated and discussed using both geometrical and structural parameters as design variables and different choices of the multiconstrained objective function.

List of symbols

DBobs k	noise level for observer k	R	rotor radius
F	objective function	T_{ave}	average pitch link load
F_{x_j}	1 / 2 peak to peak hub force in the x_j direction	$T_{1/2ptp}$	1 / 2 peak to peak link load
g	inequality constraint	v	velocity
h	equality constraint	x_j	nonrotating shaft frame of reference axis
M_{x_j}	1 / 2 peak to peak hub moment in the x_j direction	$\underline{X}$	design variables vector
p	design point	w	weighting factor
P	total power	z	altitude
r	radial coordinate		

Introduction

Numerical optimization has been given considerable attention by industries during the recent past years and much progress has been made both in mathematical algorithms and in application complexity.

It has been proved that a human being cannot simultaneously and efficiently manage more than six or seven decision variables; therefore, since a general design configuration may have a much higher number of design parameters, the use of numerical techniques is mandatory in order to achieve a high level of design quality.

A wide variety of algorithms have been developed to make the numerical optimization process more and more efficient. Gradient based optimizers with finite difference gradient computations represent a well assessed field [17] [18] and many computer codes were developed using these techniques in the past decades. More recently other algorithms have been proposed. Methods using adjoint matrix operators with continuous or discrete sensitivity analysis such as control theory [14], one-shot method [15], automatic differentiation techniques [23], or methods based on the evolution theories such as genetic algorithms [13] [24], have been successfully applied to fixed wing and

airfoil aerodynamic design. The main factor linking most of these methods is that their efficiency is high only if the algorithm is dedicated to a particular class of problems.

Aerodynamic rotary wing design using automatic design procedure is not so mature as the fixed counterpart due to the intrinsically greater complexity of the flow phenomena and the higher level of multidisciplinary analysis required by the issue, which involves aerodynamics as well as dynamics, acoustic and structures. The objective of advanced design is to obtain performance improvements together with a reduction of vibration and noise level. However, to make the numerical optimization process practicable in terms of computer power, a compromise must be chosen between the level of complexity of the mathematical model used in the multidisciplinary analysis and a realistic representation of the flow field as well as the aeroelastic behaviour of the blades.

The standard of reference of aerodynamic and dynamic analysis codes used for numerical optimization applications in helicopter industry is CAMRAD/JA. Many successful applications in rotor blade design using this level of analysis can be found in literature [1] [2] [3] [5] [9] [10] [11] [12], but very few of them show three-dimensional transonic blade optimizations using comprehensive rotor analysis codes coupled with three-dimensional full potential rotor codes [7] [8]. Comparing these tools to the fixed wing design ones, which now begin to be practicable also with 3D Euler [14] or even 3D Navier-Stokes solvers [16] [23], we cannot but notice a great gap between the former and the latter, although widely justified by aerodynamic phenomena and numerical problems of more complexity and delicacy.

In order to have a constrained function minimization algorithm of general applicability, with a realistic potential of improvement in the future, the selected technique, developed and used for the applications illustrated in the present paper, is a hybrid technique based on a Genetic Algorithm (GA) and a Feasible Direction Method (FDM). This approach looks attractive in view of GA great potential to deal with a very wide range of issues without being specifically dedicated to a particular analysis solver, its capability to reach the global optimum point in discontinuous and/or multimodal spaces managing also discrete variables and its high level of parallelization for supercomputer calculations. The feasible direction optimizer could further accelerate the convergence ratio towards the optimum configuration thanks to its higher efficiency in local refinement close to search hyperspace extremal points. Applications of a Genetic Algorithm in rotor blade design for noise reduction can be found in [6].

The aforementioned optimization algorithms have been created and integrated into a general purpose design tool (DESPOTA, DESign Procedure using OpTimization Algorithms) for helicopter rotor blades using both CAMRAD/JA and an Agusta proprietary code as comprehensive analysis codes.

This paper presents some results of rotor blade multi-point design obtained through multidisciplinary analysis for performance improvement and for noise and oscillatory hub reaction components reduction applied to a twin engine helicopter of the same class as Agusta A109C helicopter.

1. The optimization problem

The general statement of an optimization problem can be summarized as follows:

Minimize:	$F(\underline{X})$		(objective function)
	$g_j(\underline{X}) \leq 0$	$j = 1,m$	(inequality constraints)
Subject to:	$h_k(\underline{X}) = 0$	$k = 1,l$	(equality constraints)
	$X_i^l \leq X_i \leq X_i^u$	$i = 1,n$	(side constraints)

1.1 Feasible direction method

The method used is based mainly on the work by G. N. Vanderplaats explained in [17]. It substantially adopts different techniques according to the evaluation of the various constraints being considered (fig. 1). If the constraints are not active, i.e. they are far from the boundaries of the prescribed tolerance, it is possible to choose the search direction between a steepest descent and a conjugate direction or use variable metrics (ranging from DFP to BFGS). In case some constraints are active but not violated, the search direction found by the Feasible Direction Method might be tangent to some constraint hypersurfaces. In this case, it is possible to prevent violation of non convex constraints choosing either an algorithm adopting some push off factors to leave the constraints boundaries or to split the design variables into dependent and independent, using a Newton algorithm to follow the active constraint hypersurface. If one or more constraints are violated, push off factors permit to find the search direction that recovers the design in the feasible hyperspace with the minimum penalization of the objective function. If the Kuhn-Tucker

condition has not been satisfied, the one-dimensional search is then performed until a minimum is found or new constraint boundaries are met. After that, a new Jacobian of the objective function and constraints is computed to try to go on with the optimization process; otherwise each component of the objective function gradient is specifically examined until a completely negative result is obtained. Gradients are computed with finite difference steps and the 1 D search adopts a parabolic interpolation between points to look for minima.

1.2 Genetic algorithm

The Genetic Algorithm used in this paper is similar to classical GA [13] but uses a different selection process and a different alphabet, integers instead of binary. The general schema is shown in fig. 2.

A fixed number of individuals is evolved for a given number of generations by means of selection, cross-over and mutation. The criteria by which the process is guided is the level of fitness evaluated for each individual in the following generations and constraints violations. While traditional selection schemata allow to select an individual within the whole position, local geographic selection is based on the idea that the population has a particular spatial structure. It is divided into demes or semi-isolated sub-population, with relatively high gene mixing within the same deme, but restricted gene flow between different demes. One way in which demes can be created in a continuous population and enviroment is isolation due to distance: the probability that two individuals will mate is a fast declining function of their geographical distance [26].

To simulate this schema, individuals are placed on a toroidal grid with one individual for grid location. Selection takes place locally on this grid. Each individual competes with its nearby neighbours. Specifically, an individual finds his mate during a random walk starting from his location: the individual with the best fitness value is selected. Local selection has been adopted mainly because of its applicability to multi-objective optimization. It represents, in fact, a niching technique, whose aim is to maintain a useful form of diversity in the population [27]. In this sense, it is an alternative to the fitness sharing techniques [19]. Local selection has been preferred to the use of sharing techniques as it should naturally create niches without the need for problem-dependent parameter tuning.

As for the cross-over, a two point crossover operator has been used to improve GA search, as suggested in [25].

Finally, the mutation operator acts at random changing the value of a chromosome gene.

The genetic algorithm described in this paper takes into account constraints violation through a very heavy penalty introduced into the objective function. The use of a penalty function using less stringent constraint values is sometimes recommended as it often leads to more efficient optimization processes.

1.3 Hybrid technique

A simple evaluation of convergence during the evolutive process of successive generations stops the Genetic Algorithm and starts the Feasible Direction one. This evaluation can be an established percentage of improvement in the objective function for a prefixed number of generations. When using this procedure it is recommended not to insist on too much refined improvement and to sample the search hyperspace into relatively coarse discretization in order to improve the convergence ratio towards approximated minima. However, parameter tuning is generally dependent on the specific application and on the relevant level of complexity (analysis code, population size, constraints, etc.).

2. Analysis codes

Three main rotor analysis codes were involved in this work: NFCNTL, NOISE (Agusta proprietary codes) and CAMRAD/JA.

NFCNTL [22] is a blade element code that allows to evaluate, knowing the control angles or the desired forces in the shaft reference system, all the rotor quantities: power, flapping and lagging motion for any rotor attitude in space.

This code provides first of all the correct equilibrium between thrust and induced velocity, and then evaluates the resulting flap motion. The iteration procedure is repeated until the desired tolerance is obtained for all the controlled parameters. A first order approximation of the gradients is used to obtain the target forces in the shaft reference system.

The program is particularly dedicated to the prediction of the torsional loads at the blade root, in order to provide an important indication for a correct dimensioning of the flight control system already in earlier design stage.

Aerodynamic characteristics of the airfoils distributed on the blade are provided in tabular form as coefficients vs Mach number and angle of attack (up to five different airfoils along the blade).

The simple uniform inflow or the more complex Mangler and Squire or Glauert models for the induced velocity are used and a procedure from Ericsson theory accounts for the unsteady effects.

This code has been extensively tested with Agusta flight tests data, obtaining positive results, despite its relative simplicity (for example only a rigid blade motion is assumed).

The method used for the acoustic prediction in NOIS code is based on a simplified integration of the Ffowcs Williams-Hawkings equation which permits to evaluate the thickness and the loading noise in the time domain relative to observers fixed in space or moving independently with respect to the helicopter. The time hystories are then transformed in 1/3 octave band SPL data and standard evaluation of ground reflection and atmosphere absorption are taken into account. The results are finally expressed in dBA.

CAMRAD/JA [20] [21] is one of the most used comprehensive analysis tools in helicopter industries. Aerodynamic loads are computed in compliance with the lifting line theory, using steady two-dimensional airfoil aerodynamic coefficients and a vortex wake. It can take into account unsteady and compressibility effects, yawed flow, Reynolds number, swept wing, lifting surface corrections and dynamic stall with several models. The nonuniform inflow analysis is based on a prescribed wake geometry, subsequently relaxable to better predict the actual wake development. This analysis is not available for hover conditions, for which only empirical inflow models are used. BVI is taken into account by a second order lifting line or by a lifting surface or by an artificially large vortex core radius. An interface to CFD rotor codes is available through files interchange of partial inflow angles and rotor loads computed by threedimensional transonic analysis. This allows to better simulate the true three-dimensional transonic unsteady effects at the blade tips in the advancing side of the rotor disk, which are not negligible at high forward flight speed. Agusta has developed an unsteady full potential rotor code and interfaced it with CAMRAD/JA for transonic analysis in trimmed flight conditions (UTARCAM code), but at the present time activation of this routine in optimization problems is at a very preliminary stage. The rotor structural model is based on engineer beam theory for rotating wings with large pitch and twist. The rotor blade is assumed to have a straight, undeformed elastic axis, with specified blade root possibilities. The dynamic model adopts an approach based on rotating, free-vibration modes, equivalent to a Galerkin analysis, which can be computed internally or as input data. In addition, this tool allows to perform other kinds of analyses, as, for example, a linear stability analysis for gust response and flutter or the calculation of the thickness and loading far field rotational noise with respect to observers fixed to the rotor mast.

3. Applications

Three design examples of main rotor optimization have been performed for both performance improvement and noise reduction. The first one also considers pitch link load reduction, whereas the latter takes into account the oscillatory (1/2 peak to peak) component reduction of the hub reactions in the nonrotating reference frame. These components alone do not give a full indication of vibration level yet, as both the phases with which they go into the airframe and the airframe response and interaction play an important role in the vibratory level at a given point of the rotorcraft. However, at present no vibration level in some characteristic point or empirical vibratory indices have been included in the objective function, and only purely reduction of a weighted sum of the hub oscillatory (1/2 ptp) reaction components in the nonrotating reference system have been considered.

The selected test cases relate to a twin engine light helicopter of the class of Agusta A109C (four blade main rotor) and have been run on HP Apollo 720 and on SGI Indigo2 workstations.

3.1 Rotor modelling

If not specified otherwise, both NFCNTL and CAMRAD/JA rotor models used for the following examples have a subdivision of the blade into 24 aerodynamic segments and into 48 structural segments. Investigations of the optimal values of input parameters have been made in order to provide sufficiently accurate output without compromising the computational time required. After some investigations with NFCNTL-NOISE, the Glauert wake model has been preferred since the Mangler one slows down the convergence of the circulation and/or the flap motion at very high forward flight speed and in extremely not conventional blade planform which the Genetic Algorithm can frequently generate especially in the first generations. Similar considerations can also be made as for optimizations using CAMRAD/JA code with elastic blades and nonuniform analysis. The vortex wake model requires a very careful choice of the several wake control parameters, which are usually condition and configuration dependent. Fine tuning can be performed resorting to experimental data, a data base or experience. At time no parameter adjustment for substantial geometrical modifications is taken into account, as that is not indispensable when high speed forward flight design points are considered because vortex wake inflow effects are not so important as they are at lower flight speeds.

Rotor forces and mast orientation have been obtained from the trim of a 2850 Kg helicopter with a conventional swept back tip of the main rotor blade. The trim of the isolated main rotor in the optimization processes has been obtained using both the collective pitch and the two cyclic pitch components as control variables.

The range of the variations of the decision variables have been chosen in order to explore a large design space, but limited to reasonably buildable blade shapes. Composite materials offer a high degree of freedom from that point of view, limited practically only by manufacturing costs.

The structural congruence due to geometrical modifications is obtained acting on the rotation of the blade section inertial principal axes (inertial twist) if there has been a change in aerodynamic twist and on the positions of the gravity and the tension centres following to the sweep angle and chord distribution variations. Changes of the steady and unsteady aerodynamic centres are taken into account for geometrical and airfoil distribution modifications but variations in the section polar moments of inertia with respect to the elastic axis are not considered. A multilevel decomposition of the optimization process [4] [16] looks very interesting for a future improvement of the design methodology being presented. In such a way it is possible to structurally dimension the blade sections and compute the blade sectional structural properties required to satisfy prefixed maximum stresses and other imposed constraints (weights, thickness, stiffness, ...), which otherwise should be somehow extrapolated from the initial data.

A simplified approach to structural congruence can raise questions about, for instance, the repositioning of the best fit axis of the blade section shear stress centre for very distorted blade geometries, used by CAMRAD/JA as an elastic axis. At present, little experience has been achieved in blade aeroelastic optimizations allowing significant geometrical changes. The application on an elastic blade with planform and twist modifications being presented in this paper relates to a tip blade optimization to reduce power, noise and the oscillatory parts (1/2 ptp) of the hub reactions in the nonrotating shaft frame, with limited variations of the independent geometric variables. The rotor motion analysis in this application has taken into account five harmonic components; the blade vibratory solution has considered five flexional and two torsional degrees of freedom.

To summarize, the design tool created with CAMRAD/JA allows to choose as geometric decision variables chord, aerodynamic sweep and twist distributions along the blade. The available structural variables are the two components of the flexional stiffness together with the torsional one, the inertial twist and the gravity centres distributions. Variable airfoil distribution is also possible for both NFCNTL and CAMRAD/JA interfaces.

Both the geometric and the structural variables are modelled with a composition of Bezier splines. The order of the segments of the Bezier curves may range from one (linear variation) to three (cubic variations) according to the number of control poles that have been fixed. High sensitivity pole positions for the objective function and the constraints have been chosen taking advantages in the numerical process. To improve the modelling of high local variation, no tangent continuity is imposed between the segments of the composite curve. The radial position of the point at which the successive segment starts can be chosen as decision variable as well. The abscissa poles coincide with some stations of the radial discretization of the blade both for aerodynamic and structural quantities. The ordinates of the Bezier curves may act as global values of the related quantities or as perturbation components.

3.2 Test cases description

Each design has been performed with the FDM, the GA and the hybrid technique GA+FDM.

The number of individuals in each population for the GA optimization is fixed to 64 in all the test cases. The probability for the cross-over and the mutation operations have been set to 0.75 and 0.05 respectively.

A reference blade has been considered for each design to compare the obtained results in terms of objective function component reductions; the aforementioned blades have also been considered as the starting configuration for the FDM optimizations.

3.2.1 Design 1

The first design (D 1) has been performed using NFCNTL and NOISE codes choosing three design points. As for the first two points the aim was to reduce the total power required as well as the pitch link loads, imposing constraints onto the (approximated) maximum thrust developed by the rotor and onto blade weighted solidity, whereas for the third one the objective was to reduce the aeroacoustic noise level.

The design points are listed below.

p1) Forward flight at v=160kts and z=1000m ISA
p2) Hover at z=2000m ISA + 20° C
p3) Hover at z=0m ISA

The last design point has been included as it is more representative for noise level reduction. Two observers have been considered: the former has been positioned in the hub plane at 30m from the hub itself, whereas the latter at 30m from the hub in its plane and 14m in the vertical direction below the hub.

The objective function has the form

$$F = \sum_{1}^{2} w_i P_i + w_3 (T_{1/2ptp})_1 + \sum_{1}^{2} w_{3-i} (T_{ave.})_i + w_6 (DBobs1)_3 + w_7 (DBobs2)_3$$

Constraints on rotor trimmed collective pitch and adimensional thrust over weighted solidity have been set for p1 and p2, admitting a 7% variation of the corresponding values of the reference blade. A minimum value of the maximum thrust and thrust derivative past collective pitch calculated at zero flapping have been put as constraints at 95% of the reference value; these constraints give an index of manouver capability at high forward flight speed with low computational time consumption.

Noise upper bounds equal to the values obtained for the reference blade have been established, even though noise level has been included in the objective function, too.

The reference blade has a rectangular planform up to r/R=0.95 where a linear 45° leading edge swept back tip with a taper ratio equal to 0.33 starts. Twist is piecewise linear along the blade with a constant value in the tip region. Three basic airfoils are placed along the blade with a limited evolutive region between each other consisting of the lower and upper stations of the blade discretization with respect to the airfoil placements. The first airfoil has a 12% thickness and goes from the blade root to r/R equal to 0.87. The second one, of 9% thickness, ends at r/R equal to 0.96. The remaining part of the blade is constituted by 7% thickness airfoil sections.

The 21 decision variables are the following:

a) maximum radial position of the limiting station of the two external airfoils (2)
b) radial abscissa of the initial tip region (1)
c) chord distribution (6)
d) twist distribution (6)
e) leading edge geometry (6)

A composite Bezier spline of two segments has been considered for each of the three last groups of variables, the first segment being cubic, the second one parabolic. The abscissa of their common pole is equal for all of them and coincident with variable "b".

The variables from "c" to "e" were free to act from the beginning of the rectangular portion of the reference blade, while variable "b" has been given only a limited variation over the reference value. Side constraints for variable "a" have been set to [0.40;0.90] and [0.70;1.0] respectively.

3.2.2 Design 2

The second design (D 2) has been carried out using CAMRAD/JA code.

The objective function for this application is based on performance. Noise upper bounds have been fixed for design point 2. The blade has been supposed to be rigid and the free wake model has been used for the analysis during the optimization procedure.

The two design points are the following:

p1) Forward flight at v=160kts and z=1000m ISA
p2) Hover at z=2000m ISA + 20° C

The objective function has the form

$$F = \sum_{1}^{2} w_i P_i$$

Inequality constraints have been fixed for the collective pitch, adimensional thrust over solidity, an averaged and a maximum section angle of attack in the most critical sector of the retreating side of the rotor disk for r/R>0.51 in p1. The first two quantities admit a variation of maximum 7% while the latter ones have been set at values of 2° lower than those computed for the reference blade.

Noise upper bounds have been set in p2, positioning two observers at 30m from the hub in its plane and in a 45° inclined plane. The values are 0.5% higher than those computed for the reference blade.

The reference blade has a rectangular planform up to r/R=0.95 with a linear 45° quarter chord swept back tip. Radius and twist distribution is the same as in design 1 reference blade, blade solidity is lower and taper ratio is augmented to 0.37; airfoil thickness and distribution is the same, too, except that the limit stations of the 12% and 9% thickness airfoils are r/R=0.85 and r/R=0.95 respectively. As this design has been deliberately set within the unfeasible search hyperspace (because of the angle of attack distribution), the result obtained through the FDM optimization is useful to measure the recover feature built into FDM in the feasible hyperspace under the given conditions.

The 17 decision variables (for D 2.1) are:

a) maximum radial position of the limiting station of the two external airfoils (2)
b) radial abscissa of the initial tip region for the chord distribution (1)
c) chord distribution (6)
d) aerodynamic twist distribution (4)
e) aerodynamic quarter chord sweep distribution (4)

A composite Bezier spline of two segments (3° and 2° order) has been considered for variable groups "c", while a simple cubic one has been adopted for group "d" and "e". Only group "c" and "d" acted on the whole blade, while "e" did from r/R>0.85. Side constraints for variable group "a" are *[0.60;1.0]* and *[0.70;1.0]* respectively.

A moderate variation of aerodynamic sweep is allowed up to r/R=0.92 in order to bound excessive aeroelastic negative phenomena for the optimized blade.

The same design problem has been studied with fixed airfoil distribution (D 2.2).

3.2.3 Design 3

The third design (D 3) has been performed using CAMRAD/JA code with elastic blade modellization (41 inertial stations) and the free wake model (22 aerodynamic segments).

The goal is to reduce power consumption, noise (in hover) and the oscillatory (1/2 ptp) components of the hub reactions in the non rotational frame for the forward flight design point.

The two design points are

p1) Forward flight at v=150kts ISA
p2) Hover at z=0m ISA

The objective function is:

$$F = \sum_{1}^{2} w_i P_i + \sum_{1}^{3} w_{2+j}(F_{x_j})_1 + \sum_{1}^{3} w_{5+j}(M_{x_j})_1 + w_9(\mathrm{DBobs1})_2 + w_{10}(\mathrm{DBobs2})_2$$

Upper inequality constraints have been set on the total power required in p1 and noise level in p2 for two observers positioned as in design 2. These constraint values are respectively 0.5% higher and equal to the ones computed for the reference blade. The angle of attack distribution has been constrained as in design 2 with upper constraints corresponding to the values calculated for the reference blade.

The reference blade has a higher rotational speed and a lower rotor radius in comparison with those of designs 1 and 2. The tip is parabolic, starts at r/R=0.94 and has a 0° sweep angle at the trailing edge. Aerodynamic twist is linear along the whole blade without slope discontinuities. Airfoil thickness is 11% up to r/R equal to 0.87 and 7% outside. Tip centre of gravity distribution has been supposed to be placed slightly ahead of the middle of the corresponding tip chords. The aforementioned blade does not present aeroelastic instability in the speed range of the rotorcraft.

The 15 decision variables act only in the tip region and are the following:

a) chord distribution (4)
b) aerodynamic twist distribution (3)
c) aerodynamic quarter chord sweep distribution (4)
d) centre of gravity distribution (4)

Since sweep of the 1/4 chord line has been subjected to limited variations with respect to the reference blade values and negative values have not been allowed, it is reasonably possible not to consider variations of the elastic axis angle (set at 0°); in addition, sections polar moment of inertia with respect to this axis have not changed their values, although this hypothesis is not completely justified.

The aim of this exercise is to examine the possibility to design interchangeable tips, each one being optimized for a particular mission. A GA multiobjective optimization can lead in a single run to a final population of dominant individuals (Pareto front) with respect to a continuos variation of the weighting factors of each objective function component.

4. Results and discussion

Power required and loads improvements of the optimized blades are expressed in terms of percentage reductions of the corresponding reference value, whereas noise level reductions are expressed in dBA values. Tables for design 1 also show the total power variation in p3, whereas tables for design 2 represent the variations of total, profile and induced power obtained, for the same configuration, with both the free wake model used in the optimization process and the uniform inflow one.

4.1 Design 1

Obj funct. eval.: 236	Total power	Noise obs. 1 (abs. diff.)	Noise obs. 2 (abs. diff.)	Average load	1/2 peak to peak load
p1	9.25			19.72	5.27
p2	4.90			47.91	
p3	5.27	2.19	3.32		
The 12% thickness airfoil extends up to r/R=0.57 and the 9% one up to r/R=1.0					

Tab. 1 : % Reduction obtained with FDM

Obj funct. eval.: 1920	Total power	Noise obs. 1 (abs. diff.)	Noise obs. 2 (abs. diff.)	Average load	1/2 peak to peak load
p1	10.75			1.99	18.75
p2	11.28			39.61	
p3	14.52	7.65	6.57		
The 12% thickness airfoil extends up to r/R=0.48 and the 9% one up to r/R=1.0					

Tab. 2 : % Reduction obtained with GA (30 gen.)

Obj funct. eval.: 901	Total power	Noise obs. 1 (abs. diff.)	Noise obs. 2 (abs. diff.)	Average load	1/2 peak to peak load
p1	11.39			- 1.18	20.76
p2	11.54			39.72	
p3	15.00	8.04	6.79		
The 12% thickness airfoil extends up to r/R=0.44 and the 9% one up to r/R=1.0					

Tab. 3 : % Reduction obtained with GA (12 gen.) + FDM

Obj funct. eval.: 1749	Total power	Noise obs. 1 (abs. diff.)	Noise obs. 2 (abs. diff.)	Average load	1/2 peak to peak load
p1	11.15			- 10.30	27.21
p2	11.09			29.74	
p3	14.05	7.69	6.64		
The 12% thickness airfoil extends up to r/R=0.45 and the 9% one up to r/R=1.0					

Tab. 4 : % Reduction obtained with GA (24 gen.) + FDM

Tables. 1-2-3 show the results obtained with the different optimization techniques described in this paper. Table 4 is an example of FDM applied to the best blade obtained after a number of generations doubled with respect to the number of those corresponding to the convergence for the hybrid optimization process. The value of the objective function of this final blade is not so satisfactory as the one obtained in table 3. The FDM optimization alone has given results not as good as those obtained using GA, because it has stuck at a local minimum. The best blade obtained with GA after 30 generation does not show any substantial improvement in comparison with that obtained after 24 generation, while the average fitness value of the population of that generation does, indicating a further general improvement in the quality of the progressive blade populations. Applying FDM after 12 generations has led to a 2% reduction in total power required and noise level, as well as a general 10% reduction in control loads; these improvements have been obtained leaving airfoil distribution practically unchanged. Optimized blade chord, twist and planform are shown in fig. 3. The general trend is to increase the chords in the first 2/3 of the blade span, twist them in the first 1/3 and decrease them in the outboard region. The lift coefficient and angle of attack distribution show that the optimized blades support higher loads in the medium sections and lighter loads in the external ones, thus reducing the drag coefficient for most of the effective portion of the blade span thanks also to the much more internal section where the 9% thickness airfoil starts. The 7% thickness airfoil has completely disappeared from all the final blades, replaced by the next thicker one; this is probably due to a better load distribution in the retreating side of the rotor disk that allows the blade to work farther from the stall thanks to higher maximum lift coefficient and lift curve slope of the 9% thickness airfoil reducing the oscillatory control load component. The greater extension of the 9% thickness airfoil allows a significant taper of the blades in their 1/3 final region without violating constraints of maximum thrust and weighted solidity, but rather causing them to shift at the minimum and maximum values respectively allowed by constraints. Reduced chords and better smooth sweep angles distribution partially balance the higher drag coefficient (at low lift coefficient and high Mach number) of the 9% thickness airfoil with respect to the 7% one.

4.2 Design 2

D 2.1.1	Obj funct. eval.: 153	Total power	Induced power	Profile power	Noise obs 1 (abs diff)	Noise obs 2 (abs diff
p1	free wake	12.14	6.97	23.59		
	uniform	7.27	0.65	13.82		
p2	uniform	1.98	0.10	10.51	2.50	- 0.42
The 12% thickness airfoil extends up to r/R=0.63 and the 9% one up to r/R=0.70						

Tab. 5 : % Reduction obtained with FDM

D 2.1.2	Obj funct. eval.: 1920	Total power	Induced power	Profile power	Noise obs 1 (abs diff)	Noise obs 2 (abs diff
p1	free wake	9.59	0.48	21.31		
	uniform	6.76	- 0.97	12.72		
p2	uniform	2.37	0.09	12.74	4.46	0.97
The 12% thickness airfoil extends up to r/R=0.60 and the 9% one up to r/R=0.76						

Tab. 6 : % Reduction obtained with GA (30 gen.)

D 2.1.3	Obj funct. eval.: 604	Total power	Induced power	Profile power	Noise obs 1 (abs diff)	Noise obs 2 (abs diff
p1	free wake	12.28	5.14	24.54		
	uniform	11.85	0.04	22.59		
p2	uniform	2.87	0.07	15.64	3.63	0.48
The 12% thickness airfoil extends up to r/R=0.60 and the 9% one up to r/R=0.70						

Tab. 7 : % Reduction obtained with GA (8 gen.) + FDM

D 2.2.1	Obj funct. eval.: 136	Total power	Induced power	Profile power	Noise obs 1 (abs diff)	Noise obs 2 (abs diff
p1	free wake	4.55	6.63	7.15		
	uniform	2.78	0.64	5.29		
p2	uniform	1.17	0.13	5.91	1.89	- 0.06
Airfoil distribution fixed and coincident with that of the reference blade						

Tab. 8 : % Reduction obtained with FDM

D 2.2.2	Obj funct. eval.: 1920	Total power	Induced power	Profile power	Noise obs 1 (abs diff)	Noise obs 2 (abs diff
p1	free wake	3.64	- 1.56	8.98		
	uniform	3.11	0.77	5.99		
p2	uniform	1.06	0.00	5.88	1.65	- 0.21
Airfoil distribution fixed and coincident with that of the reference blade						

Tab. 9 : % Reduction obtained with GA (30 gen.)

D 2.2.3	Obj funct. eval.: 874	Total power	Induced power	Profile power	Noise obs 1 (abs diff)	Noise obs 2 (abs diff
p1	free wake	5.62	3.40	10.80		
	uniform	4.84	0.82	9.23		
p2	uniform	1.69	0.05	9.10	2.62	0.50
Airfoil distribution fixed and coincident with that of the reference blade						

Tab. 10 : % Reduction obtained with GA (10 gen.) + FDM

This test case is useful to understand the extent of performance improvements due to modified airfoil distribution when acting simultaneously on blade planform and aerodynamic twist.

Chord and twist distributions and blade planform obtained in design 2 are shown in fig. 4 and fig. 5, for variable and fixed airfoil distribution respectively. D 2.1 designs (variable airfoil distribution) differ from D 2.2 (fixed airfoil distribution) in the following:

1) larger blade central region
2) greater twist (not relating to D 2.2.1)
3) opposite twist curvature distribution in the outboard region
4) lower tip area (except for D 2.1.1)

Differences 1) and 2) are due to the lower lift generated at high angles of attack at moderate Mach numbers by the 7% thick airfoil extending inboard up to 0.70-0.76 r/R in D 2.1. This causes the blade to balance the request for high lift coefficient (at angles of attack lower than constraint bounds) in the retreating side of the rotor disk, enlarging the chords in its central region.

Twist distribution makes the blade more loaded in its inboard region in the advancing side of the rotor disk when fixed airfoils are considered, does allowing the thicker airfoils to work at better angle of attack distribution and lower drag coefficient in the 1/3 external region if compared with those of the reference blade.

A common and important mechanism to reduce power is to smooth the 1/4 chord line sweep angle close to the tip crank reducing the peak in the profile power coefficient in the critical advancing sector of the rotor disk in p1.

Noise level variations shown in the above tables demonstrate that a substantial reduction can be obtained without specifically including it in the objective function even with fixed airfoils. These improvements come from a better load distribution in the rotor disk in the high Mach number region and a lower blade section area obtained with respect to the reference blade.

In this test case, the Genetic Algorithm alone demonstrated less efficiency than FDM alone. The reason for this difference is probably due to GA calibration for an hybrid optimization causing less efficiency with respect to its potential, but a more rapid convergence, which was required for the hybridization with a gradient based optimizer.

Tip areas of D 2.2 are higher than those of D 2.1, though they have thicker airfoils. This behaviour could be explained by higher sensitivity towards area reduction in the region just inboard of r/R=0.85, which is not smoothed by swept wing effects and has high dynamic pressure with relevant compressibility effects (acting on a 12% airfoil). Further reductions of tip area could have caused constraints violation on angle of attack (always active for both final D 2.1 and D 2.1 designs) and/or worsened the objective function value.

4.3 Design 3

Obj funct. ev.: 166	Total power	F_{x_1}	F_{x_2}	F_{x_3}	M_{x_1}	M_{x_2}	M_{x_3}	Noise obs. 1 (abs diff)	Noise obs. 2 (abs diff
p1	1.13	- 9.10	90.41	- 15.94	51.46	32.18	- 15.73		
p2	0.32							0.18	0.19

Tab. 11 : % Reduction obtained with FDM

Obj funct. ev.: 640	Total power	F_{x_1}	F_{x_2}	F_{x_3}	M_{x_1}	M_{x_2}	M_{x_3}	Noise obs. 1 (abs diff)	Noise obs. 2 (abs diff
p1	0.82	13.41	51.98	73.05	- 12.17	21.01	- 92.70		
p2	0.21							0.21	0.11

Tab. 12 : % Reduction obtained with GA (10 gen.)

Obj funct. ev.: 401	Total power	F_{x_1}	F_{x_2}	F_{x_3}	M_{x_1}	M_{x_2}	M_{x_3}	Noise obs. 1 (abs diff)	Noise obs. 2 (abs diff
p1	0.88	8.05	88.81	50.84	11.66	0.14	10.76		
p2	0.34							0.19	0.15

Tab. 13 : % Reduction obtained with GA (5 gen.)+FDM

In this design a less stringent convergence criteria for the hybrid optimization has been set having caused FDM to start after 5 generations of GA only. GA has then been performed for 5 generations more: the 10th generation best blade has turned out to be substantially different from the one obtained after 5 generations, demonstrating the general discontinuous progression of a GA optimization.

Blade tip planform, aerodynamic twist and centre of gravity distribution obtained in the present test case are shown in fig. 6. While the blade tips resulted from FDM and GA+FDM look similar, the one obtained with GA alone presents a more severe taper at the beginning of the tip region, a substantial reduction of the quarter chord sweep angle in the half outboard range of the tip with a forward shift of the sections centre of gravity and an increase in the aerodynamic (and inertial) twist in this region. Common features of all the final designs are reductions in the tip area in the first half of the tip and reductions in twist at its very beginning. Gravity centre section distributions have shifted forward in all the tip sections except in the extreme tip portion of the one obtained with FDM only.

Looking at tables 11-12-13, a general improvement in performance and noise level may be noticed, but different results have been obtained with the 1/2 ptp hub reaction components. The 1/2 ptp side force F_{x_2} in particular and the 1/2 ptp pitching moment M_{x_2} have been reduced in all the final designs, whereas the 1/2 ptp torque M_{x_3} has been augmented in all designs except that obtained with GA+FDM. A great reduction of the 1/2 ptp vertical hub load F_{x_3} has been obtained with GA and GA+FDM while FDM has led to the best result on the rolling moment M_{x_1}.

The present design has been performed in order to analyze the potential of an integrated aerodynamic/dynamic/aeroacoustic optimization using a limited combination of geometrical and structural variables active only in the tip region. Results show that helicopter vibration reductions are possible with both performance improvement and noise level reduction. To draw more accurate conclusions, a complete study should be made thoroughly modelling a specific vehicle in order to see which components of the oscillatory hub shear have the greatest influence on the vibration level in significative points of the rotorcraft and which structural variables offer the greatest efficiency to achieve a high quality design.

Conclusions and future developments

A flexible and effective tool (DESPOTA) has been developed and successful applications have been shown and discussed in multipoint rotor blade design for performance improvement, pitch link load and noise reduction, obtained acting on geometrical variables and on airfoil distribution along the blade span. A preliminary study of combined aerodynamic/dynamic/aeroacoustic optimization has been accomplished acting on both geometrical and structural variables, offering a base for further developments.

The above results suggest the following remarks:

1) The use of free wake analysis in forward flight during the optimization process can capture the geometrical modifications necessary to reduce induced power, whilst the use of uniform inflow does not. Computational time is

rather high but can be reduced limiting the analysis to the prescribed wake stage without substantially affecting the optimization trends.

2) Hover condition needs a lifting surface and a vortex wake model to take into account combined tip taper, sweep and anhedral angle distribution to further reduce rotor induced power.

3) A suitable airfoil distribution has a profile power and noise reduction potentiality as high as combined sweep, chord and twist distribution modifications.

Future developments of the described design methodology could include a blade structural analysis and a transonic analysis over the blade tip in the advancing side of the rotor disk at high forward flight design points. This last analysis can take into account the (unsteady) three-dimensional effects that could lead to wave drag increase and shock wave extension outboard of the blade causing high impulsive noise if delocalization phenomena occur. This nonlinearity has not been taken into account in the formulation of the mathematical aeroacoustic model used in this work. A full potential solver can compute the aforementioned aerodynamic effects (but not the 3D viscous phenomena in the retreating side of the rotor disk) thanks to its capability to satisfactory describe the involved flow phenomena and within an acceptable computational time (for a single analysis). Using it roughly in an optimization process is however extremely onerous, above all if it is not limited to a quasisteady 90° azimuthal blade position computation. Investigations have to be made to find out which are the best and most efficient criteria based on fluid flow properties that can be established using this kind of tool and which are the most effective decision variables in order to limit their number. Besides, it would be interesting to understand whether the 3D unsteady optimization trends can be captured by the quasisteady ones (approximated sensitivities analysis).

The optimization algorithms presented in the present work have proved to be robust, efficient and very easily applicable to other analysis solvers. On their use it is possible to state that:

1) the Genetic Algorithm is a powerful technique for global optimization especially when a good starting design for FDM is not available. Inserting superindividuals from a database in the first generation or using starting population of good average quality (for instance computed in preceding similar applications) may increase the efficiency of the optimization process leading to high quality design especially when GA is hybridized with FDM.

2) A careful use of constraints and objective function definition is highly advisable in order to avoid the use of populations with a high number of individuals and provide at the same time a sufficient variety of good genetic heritage in the first populations.

3) The Feasible Direction Method is more efficient for local refinement in comparison with GA. When a large design space with many variables is explored, the possibility to obtain better final design quality using GA is higher.

4) The hybrid optimization procedure has always been able to obtain the best quality design and can be competitive in terms of cost/effectiveness with respect of FDM only.

The developed algorithms can be improved in their performances and efficiency in many ways. The Genetic Algorithm is very suitable for multiobjective optimization and parallel implementation; a dynamic dimensioning of the populations and an improvement in the use of the genetic heritage of the generated populations could further reduce the computational time required by the optimization processes. The Feasible Direction Method might profit by automatic differentiation techniques to compute the exact sensitivity derivatives with a possible reduction of the computational time needed as well. As these techniques have in general some particular requirements in the source analysis code statements to ensure a good quality of the rebuilt analysis code and other limitations due to computer memory requirements, a careful investigation on their use on specific codes is however necessary to give correct answers.

Acknowledgements

The authors would like to thank F. Nannoni of Agusta Aerodynamic and Fight Mechanic Dept., P. Abdel Nour and P. Difrancescantonio of Agusta Dynamic Dept. for providing helpful suggestions during the accomplishment of the present work.

References

1. Walsh J. L., Bingham G., Riley M. F., "Optimization Methods Applied to the Aerodynamic Design of Helicopter Rotor Blades", Journal of American Helicopter Society, Oct. 1987.

2. Callahan C. B., Straub F. K., "Design Optimization of Rotor Blades for Improved Performance and Vibration", 47th Annual Forum of the American Helicopter Society, Phoenix, AZ, May 1991.

3. Adelman H. M., Mantay W. R., "Integrated Multidisciplinary Design Optimization of Rotorcraft", Journal of Aircraft, Vol. 28 No 1, pp. 22-28, jan. 1991.

4. Walsh J. L., Young C., Pritchard J. I., Adelman H. M., Mantay W. R., "Integrated Aerodynamic/Dynamic/Structural Optimization of Helicopter Rotor Blades Using Multilevel Decomposition, NASA TP 3465, Jan 1995.

5. Costes M., Beaumier P., Gardarein P., Zibi J., "Methods de calcul aerodynamique appliquees aux rotors d' helicopteres a l' ONERA", AGARD/FDP 75th Meeting and Symposium onAerodynamics and Dynamics of Rotorcraft", Berlin , Germany, 10-14 Oct. 1994.

6. Wells V. L., Han A. Y., Crossley W. A., "Acoustic Design of Rotor Blades Using a Genetic Algorithm", *AGARD/FDP 75th Meeting and Symposium onAerodynamics and Dynamics of Rotorcraft", Berlin , Germany*, 10-14 Oct. 1994.

7. Tauber M. E., Langhi R. G., "Transonic Rotor Tip Design Using Numerical Optimization", NASA TM 86771, Oct. 1985.

8. Hassan A. A., Charles B.D., "Airfoil Design for Helicopter Rotor Blades - A threedimensional Approach", 50th Annual Forum of the American Helicopter Society, Washington, DC, May 11-13, 1994.

9. Vuillet A., "Rotor and Blade Aerodynamic Design", AGARD R 781, Aerodynamic of Rotorcraft, 1990.

10. Friedmann P. P., "Helicopter Vibration Reduction Using Structural Optimization with Aeroelastic/Multidisciplinary Constraints - A Survey", Journal of Aircraft, Vol. 28 No 1, pp. 8-21, jan. 1991.

11. Chattopadhyay A., Walsh J. L., Riley M. F., "Integrated Aerodynamic Load/Dynamic Optimization of Helicopter Rotor Blades", Journal of Aircraft, Vol. 28 No 1, pp. 58-65, jan. 1991.

12. Davis M. W., Weller W. H., "Helicopter Rotor Dynamics Optimization with Experimental Verification", Journal of Aircraft, Vol. 28 No 1, pp. 38-48, jan. 1991.

13. Poloni C., Mosetti G., "Aerodynamic Shape Optimization by means of a Genetic Algorithm", 5th International Symposium on Computational Fluid Dynamics, Sendai, Aug 31 - Sept. 3, 1993.

14. Jameson A., "Optimum Aerodynamic Design Via Boundary Control", AGARD -FDP-VKI Special Course on Optimum Design Methods for Aerodynamics, Bruxelles, VKI, 25-29 April 1994.

15. Koruvila G., Ta'asan S., Salas M. D,, "Airfoil Optimization by the One-shot Method", AGARD -FDP-VKI Special Course on Optimum Design Methods for Aerodynamics, Bruxelles, VKI, 25-29 April 1994.

16. Borland C. J., Benton J. R., Frank P. D., Kao T. J., Mastro R. A., Barthelemy J-F. M., "Multidisciplinary Design Optimization Of a Commercial Aircraft Wing - An Experimental Study", pp. 505-519, AIAA-94-4305-CP.

17. Vanderplaats G. N., "Numerical Optimization Techniques For Engineering Design", McGraw-Hill Book Company, 1984.

18. Lasdon L. S., "Optimization Theory for Large Systems", *Macmillan Series in Operational Research*, 1970.

19. Goldberg D. E., "Genetic Algorithms in Search Optimization and Machine Learning", Addison Wesley, 1989.

20. Johnson W., "CAMRAD/JA. A Comprehensive Analytical Methods of Rotorcraft Aerodynamic and Dynamic". Johnson Aeronautics Version, Theory Manual, 1988.

21. Johnson W., "CAMRAD/JA, A Comprehensive Analytical Methods of Rotorcraft Aerodynamic and Dynamic", Johnson Aeronautics Version, User' s Manual, 1988.

22. Nannoni F., Pagnano G., Simoni M., Correlation of Flight, Tunnel and Prediction Methods Data on a Helicopter Main Rotor, paper 67, 17th European Rotorcraft Forum, Berlin, Germany, Sept. 1991.

23. Carle A., Green L.L., Bischof C. H., Newman P.A., "Applications of Automatic Differentiation in CFD", AIAA 1994.

24. Quagliarella D., Della Coppa A., "Genetic Algorithms applied to the Aerodynamic Design of Transonic Airfoils", 12th AIAA Applied Conference, Colorado Springs, CO USA, 1994, AIAA-94-1896.

25. Booker L."Improving Search in Genetic Algorithms", in L. Davis (ed.), *Genetic Algorithm and Simulated Annealing*, Morgan Kaufmann Publishers, Los Altos, USA, pp. 61-73, 1987

26. Collins R.J., Jeffersen D. R., "Selection in Massively Parallel Genetic Algorithms", Proceeding Of the Fourth International Conference on Genetic Algorithms, pp. 249-256, San Diego, USA, 1991.

27. Harik G., "Finding Multiple Solutions in Problems of Bounded Difficulty", (IlliGal Report n. 94002), University of Illinois at Urbana-Champaign, Illinois Genetic Algorithm Laboratory, Urbana, USA, 1994.

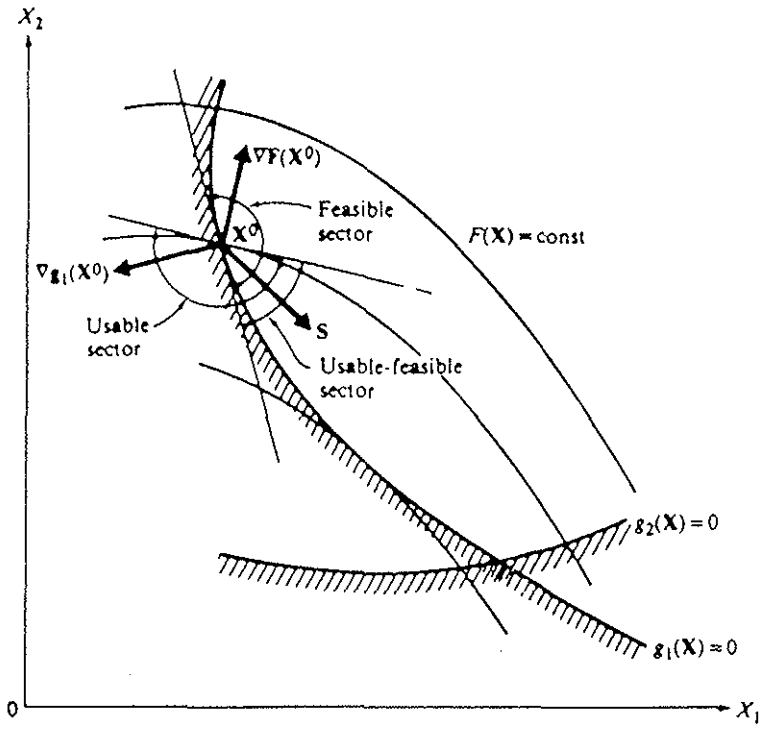

Figure 1 : Search direction in the feasible direction method

repeat

evaluate the fitness of each individual

assign to the individual the probability of extraction

repeat

extract two individuals and perform a crossover with probability pc

extract one individual and perform a mutation with probability pm

until a new generation of n individuals is completed

until a given number of generation is made or convergence is reached

	parent 1	parent 2	child 1	child 2
cross over ----->	&&&&&&	§§§§§§	&&§§§&	§§&&&§
	parent	child		
mutation ----->	&&&&&&	&&§&&&		

Figure 2 : Schema of the genetic algorithm and of the two points crossover and mutation operations

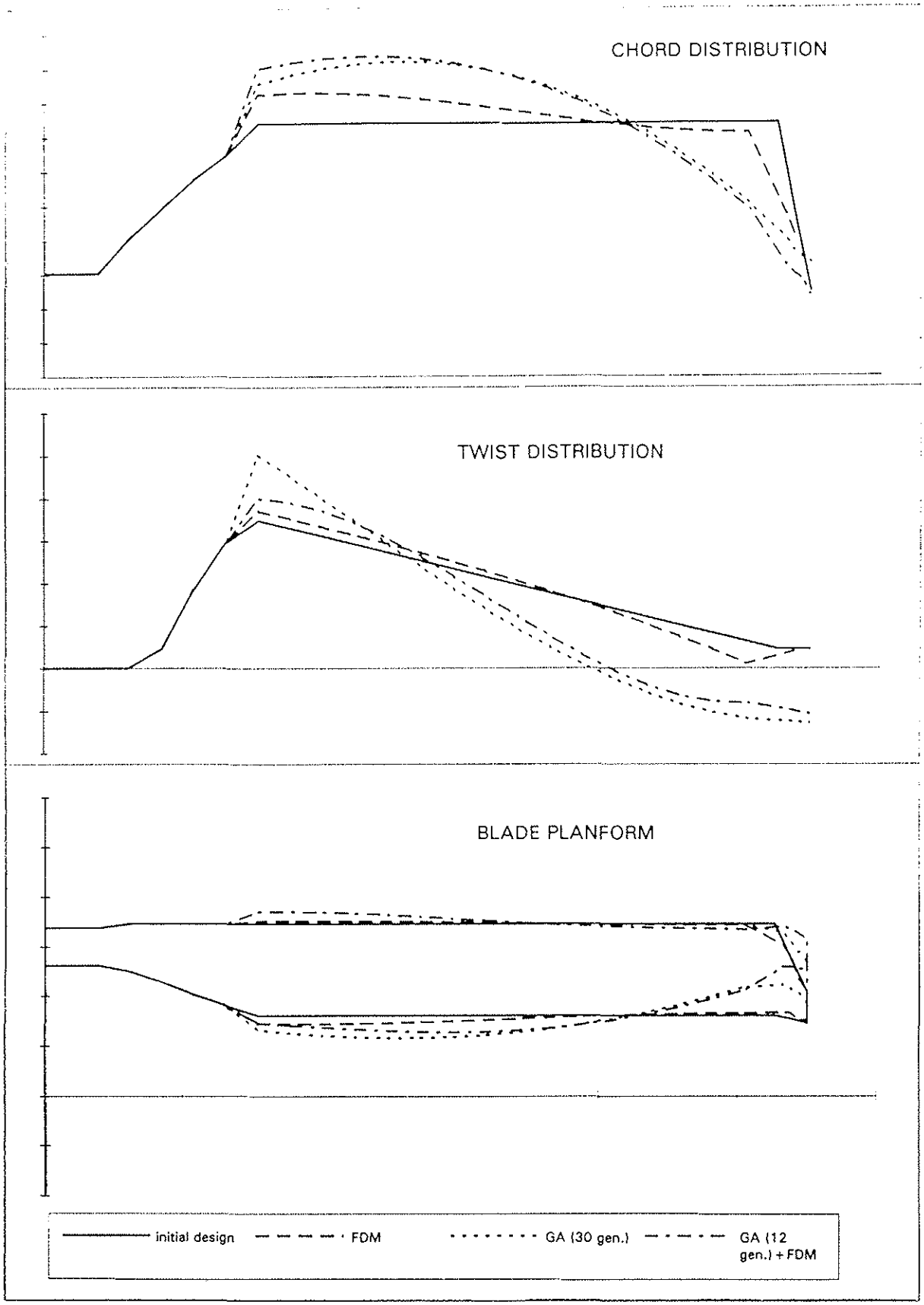

Figure 3 : Design 1 optimization with variable airfoil distribution

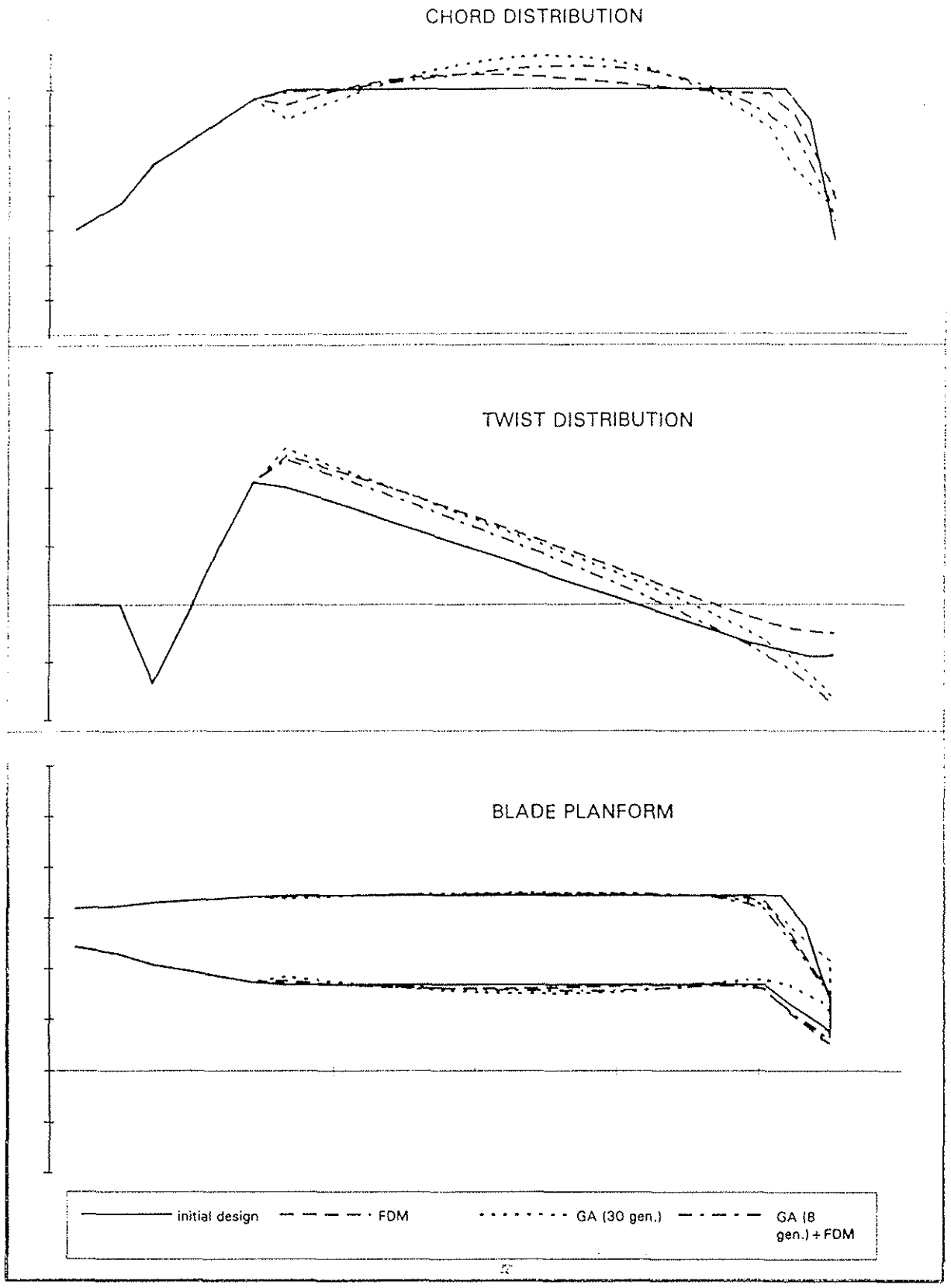

Figure 4 : Design 2.1 optimization with variable airfoil distribution

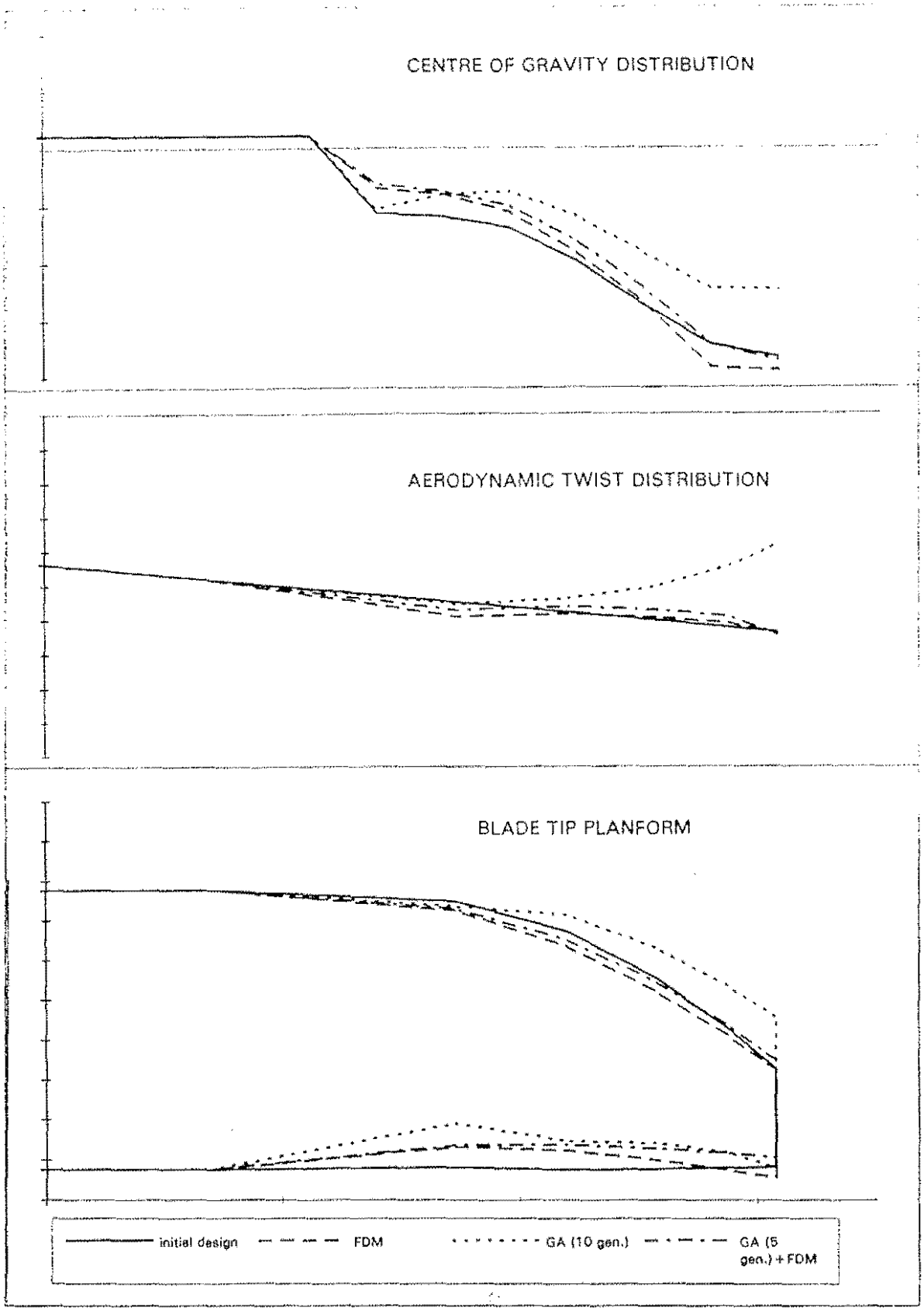

Figure 6 : Design 3 aerodynamic/dynamic/aeroacoustic optimization of a blade parabolic tip

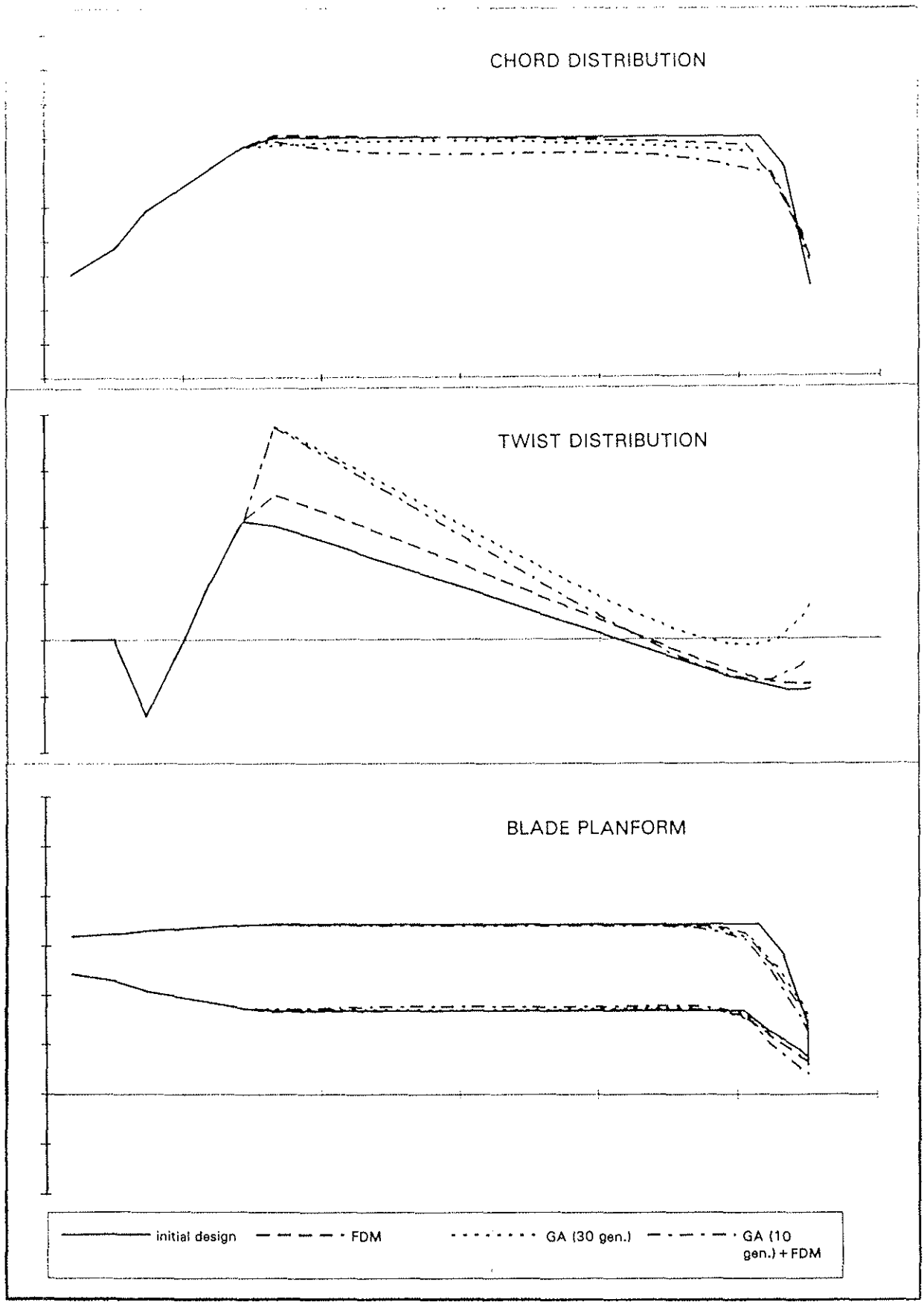

Figure 5 : Design 2.2 optimization with fixed airfoil distribution